Available online at www.sciencedirect.com
ScienceDirect
Nonlinear Analysis: Hybrid Systems 1 (2007) 81–94
Nonlinear Analysis: Hybrid Systems
www.elsevier.com/locate/nahs

Modeling dynamics of cell population molecule expression distribution

D. Milutinović[a,1], J. Carneiro[b], M. Athans[a], P. Lima[a,*]

[a] *Institute for Systems and Robotics, Instituto Superior Técnico, Lisbon, Portugal*
[b] *Gulbenkian Institute of Science, Oeiras, Portugal*

Received 28 March 2006; accepted 1 April 2006

Abstract

This article introduces a novel approach to the study of the dynamics of the molecule expression level of large-size cell populations, whose goal is to understand how individual cell behavior propagates to population dynamics. A hybrid automaton framework is used which allows the simultaneous modeling of the formation and dissociation of cell-to-cell conjugations, and the molecular processes they control. Serial encounters among the cells are described by a stochastic approach under which the cell distribution over the state space is modeled and the dynamics of the state probability density functions is determined. This work is motivated by the investigation of T-cell receptor expression distribution. These receptors are essential for the antigen recognition and the regulation of the immune system. The results are illustrated with examples and validated with real data.

Keywords: Immunology; Molecule expression dynamics; T-cell receptors down-regulation; Hybrid dynamic systems

1. Introduction

T-cells are the key regulators of the immune system and they recognize the antigen via their surface expressed molecules, so called T-cell receptors (TCRs). The antigen is presented to T-cells by specialized antigen presenting cells (APCs). The TCR expression level of a T-cell is down-regulated during the transient conjugation with an APC, which stimulates the TCRs with MHC–peptide complexes presented on the APC surface. The TCR expression dynamics of an individual T-cell involves both discrete and continuous state evolution. In this paper we describe a hybrid automaton approach [11,7,14] to modeling the TCR expression distribution in a large population of T-cells.

Available analytical models of TCR down-regulation are ordinary differential equation (ODE) models of the TCR average expression level in the population [1]. To derive such a model, partial differential equations (PDE) [19] and mean-field approaches [15] have been used. To verify such a model with data, predicted average values were compared with medians or averages of the TCR expression distributions recorded with a flow cytometry scanner [17].

* Corresponding address: Instituto de Sistemas e Robotica, Instituto Superior Tecnico, Av. Rovisco Pais, 1, 1049-001 Lisboa, Portugal.
E-mail addresses: dejan.m@duke.edu (D. Milutinović), pal@isr.ist.utl.pt (P. Lima).
[1] D. Milutinović is now a post-doc at Center for Comput. Immunology, Duke Univ. Med. Center, 2424 Hock Plaza, Suite G06, Durham 27705, NC, USA.

1751-570X/$ - see front matter
doi:10.1016/j.nahs.2006.04.003

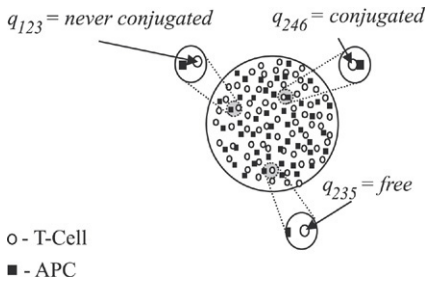

Fig. 1. The T-cell population (circles) surrounded by the APCs (squares), for the q_L discrete state of the T-cell life-cycle relating to connections to an APC. The index L is the individual cell label.

However, the recorded distributions are the result of direct observation of each individual cell, which means that a few thousand measurements are made. Considering only the average value of distributions means that lots of potentially useful information, hidden in the shape of the flow cytometry measured distribution, is discarded. To incorporate this information in a mathematical model, which relates individual cell dynamics to the observed dynamics of the population, a different approach to the study of TCR expression dynamics and similar dynamics of cell expressed molecules must be considered.

The goal of this paper is to provide a theoretical framework that will allow us to extract more information from experimentally obtained TCR expression distributions. The previous mathematical analyses [1,19,15] deal with experiments where T-cells are, under controlled conditions, always conjugated to APCs [17]. Here, we consider the data that can be obtained from *in vivo* experiments where, due to the uncertain and complex environment, the cell-to-cell conjugation and dissociation are simultaneously present and random. Sousa [16] used Monte Carlo simulations to study a similar kind of interaction between the T-cell population and APCs, and its implication for tolerance induction and the regulation of population sizes. Although this analysis provided some insight into these processes, the scope of the conclusions was limited by the lack of a full analytical model.

The paper starts with the introduction of a biological scenario in which an individual interaction between a T-cell and APCs within the cell mixture is described. On the basis of this scenario, the deterministic hybrid automaton model of an individual T-cell is introduced in Section 3. The complexity of the population interaction is discussed and it is modeled using a stochastic approach in Section 4. In the same section, the system of partial differential equations describing the probability density function of the cell state is presented. This result is exploited in the example of Section 5. In Section 6, we discuss the relation of our work to the previous studies on TCR down-regulation dynamics, and our model is validated with experimental data. Section 7 gives the conclusions.

2. Surface TCR expression level dynamics in a mixture of interacting T-cells and APCs

The scenario of interactions between T-cells and APCs is based on recent *in vivo* experiments, where the two-photon microscopy was exploited to observe the motion of T-cells inside the lymph node [10].

The minimal biological system, with the properties we are interested in, is a solution containing the mixture of T-cells and APCs (see Fig. 1). In this scenario, a naive (never conjugated) T-cell randomly moves inside the mixture. This cell is in discrete state 1 — *never conjugated*. At some instant in time, the T-cell meets an APC, and may form a conjugate if the two cells have some affinity. This can be described by the transition of the T-cell from state 1 — *never conjugated* to state 2 — *conjugated*. If conjugation happens, the T-cell is in state 2 — *conjugated* and the TCR expression level on the T-cell declines [17]. The conjugated state lasts for some time, and ceases when *dissociation* takes place. This means that the T-cell switches from discrete state 2 — *conjugated* to state 3 — *free*. After the dissociation, the free T-cell resumes random motion inside the mixture. Before conjugation to another APC, the TCR expression level can change. The T-cell can change back and forth between conjugated and free stages.

This scenario of interaction is a simplified version of experimental observations. The scenario does not include the influx of naive cells into the lymph node or the possible cell proliferation and cell death. On the other hand, in *in vivo* experiments T-cells are first labeled for the two-photon microscopy and then injected into the lymph node of the host. Experimental observations include only the live injected labeled cells that appear simultaneously in the lymph node. In the labeled T-cell population present in the lymph node, there is not an extra influx of the labeled cells. Therefore, even simplified, this scenario is completely valid at the early stage of the lymph node T-cell–APC

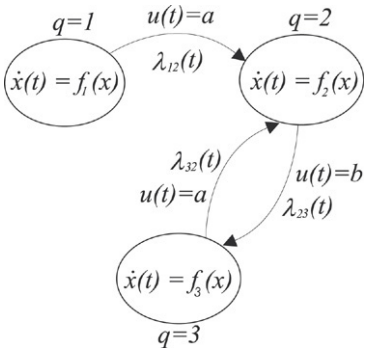

Fig. 2. Hybrid automaton model of the T-cell–APC interaction, $x(t)$ — TCR expression level, $u(t)$ — event sequence, discrete states q:1 — *never conjugated*, 2 — *conjugated*, 3 — *free*; events: a — *conjugate formation*, b — *conjugate dissociation*; $f_q(x)$ — the TCR dynamics of discrete state q, $q = 1, 2, 3$. In the case of stochastic sequences $u(t)$, the transitions are described by the stochastic rates of transition from the discrete state q to the state r, $\lambda_{qr}(t)$.

priming when the cell death and the proliferation can be neglected. On the basis of this scenario, we conclude that realistic models of TCR expression dynamics of an individual cell should take into account not only the dynamics of the TCR down-regulation, but also the sequence and dynamics of the processes of T-cell–APC conjugate formation and dissociation.

3. Hybrid automaton model of an individual T-cell

The state of an individual T-cell in the population, as regards the TCR expression level dynamics, is composed of continuous and discrete states. The continuous state (x) is related to the TCR expression, while the discrete state (q) describes whether the T-cell is conjugated to an APC or not. Thus, hybrid automata methodology appears as a natural modeling framework for the biological T-cell population.

The hybrid automaton model of the T-cell is presented in Fig. 2. Following this model, the T-cell can be in one of three discrete states: *never conjugated, conjugated* and *free*. This is a consequence of the T-cell dynamical behavior in the minimal biological system we are considering. The discrete states are introduced to model different TCR expression dynamics of the T-cell when the T-cell is naive, conjugated to APC, or free, respectively. The TCR dynamics of each discrete state is assumed to obey an ODE of the type

$$\dot{x}(t) = f_q(x), \quad q = 1, 2, 3 \tag{1}$$

where x is the TCR expression and $f_q(x)$ defines the TCR dynamics in each discrete state, $q = 1, 2, 3$, i.e., *never conjugated, conjugated* and *free* discrete state, respectively. We assume that before any conjugation, the TCR expression level remains unchanged and $f_1(x) = 0$. The dynamics of decrease and dynamics after the T-cell–APC disconnection are unknown. The only thing we know is that the consequence of the connection between the T-cell and the APC is a decrease of the TCR expression level ($f_2(x) < 0$) and that after disconnection, the TCR expression level might stay constant or be up-regulated ($f_3(x) \geq 0$).

The transitions among the discrete states are the consequence of the T-cell and the APC motion dynamics. In this modeling approach, we assume that the motion dynamics produces the time sequence of events $u(t)$ which changes the discrete state of the T-cell. This time event sequence is defined at each time instant and takes the value a, b or ε, i.e., the time event sequence $u(t)$ is a mapping

$$u : t \to \{a, b, \varepsilon\}. \tag{2}$$

The symbols a and b stand for *conjugate formation* and *conjugate dissociation* events, respectively. The symbol ε is introduced to describe *no event*, which means that the discrete state is not changing.

The T-cell hybrid system model (Fig. 2) is a deterministic model. Given an initial state (x_0, q_0) and a time sequence $u(t)$, the TCR expression level $x(t)$ and the discrete state $q(t)$ can be calculated in a deterministic way. Taking into account its deterministic nature, each T-cell model can be represented as a deterministic *single-input*, *single-output* (SISO) system (Fig. 3). The input to this system is a sequence of the events $u(t)$, and the output is the TCR expression

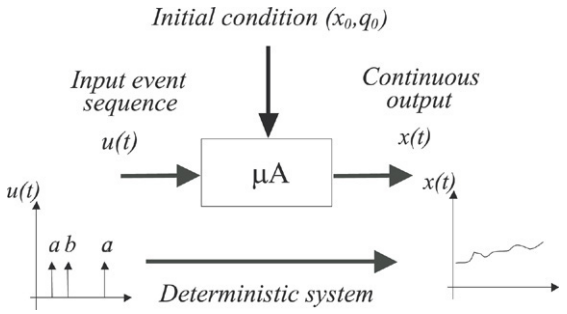

Fig. 3. Micro-agent model of the T-cell; $u(t)$ — event sequence, events: a — *conjugate formation*, b — *conjugate dissociation*; x — TCR expression level; x_0 — initial TCR expression level, q_0 — initial discrete state. In the case of stochastic event sequence $u(t)$, the expression level $x(t)$ is a continuous stochastic signal.

level $x(t)$, which is a continuous time function. This *input–output* representation will be designated as the T-cell micro-agent. The prefix "micro" is used because this model describes the population behavior at the microscopic level, i.e., at the level of the individual cell behavior. In the following section, this model will be used as a building block for the TCR expression dynamics stochastic model of the T-cell population surrounded by APCs.

A more general *multiple-output* micro-agent (μA) hybrid model is presented by the following definition:

Definition 1. A micro-agent μA is a single-input, multi-output hybrid automaton, defined as a collection $\mu A = (H, U, \tau, Y)$ where:

- H is a hybrid automaton $H = (Q, X, \text{Init}, f, \text{Inv}, E, G, R)$ that satisfies the following properties:
  - $X = R^n$, the state space of the continuous piece of H,
  - $\text{Inv}(q) = X, \forall q \in Q$, i.e., for any discrete state $q \in Q$, the invariant is the full continuous state space,
  - $G(e) = X, \forall e \in E$, i.e., all defined transitions are allowed,
  - $\text{Rs}(e, x) = x,\ \forall (e \in E \wedge x \in X)$, i.e., the transition e does not change the continuous state x,
- U is a finite set of input discrete events, including the *nil* event ε,
- $\tau : U \times Q \to E$, assigns to the pair, formed by the discrete event $u \in U$ and discrete state $q \in Q$, the transition $e = (q, q') \in E$, where $\tau(\varepsilon, q) = (q, q)$,
- $Y = R^m$ is the output state, a μA output $y \in Y$ is a function of the continuous state x, $y = g(x)$.

Remark 1. The micro-agent state is a pair $(x, q) \in X \times Q$. This couple consists of continuous $x \in X$ and discrete $q \in Q$ state components.

The properties of hybrid automaton H in Definition 1 mean that the μA discrete and continuous dynamics can evolve in a free manner (see Appendix A). However, jumps in the continuous state space part are not allowed. The previously introduced T-cell model can be derived from this abstract definition taking the *single-output* case where y is equal to the state variable x, which is the TCR expression level.

4. Stochastic model of a T-cell population

The complete population model can be derived by modeling each T-cell of the population by the T-cell micro-agent model. However, simply collecting these models will not reflect the TCR expression dynamics of the biological population. The part of the biological population complex dynamics which is not covered by this collection relates to the dynamics of the conjugate formation and the conjugate dissociation of T-cells and APCs. This complex dynamics makes an essential difference between the TCR expression dynamics of a collection of separate T-cells and the TCR expression dynamics of a T-cell biological population.

The *conjugate formation* and *conjugate dissociation* events of T-cells in the population are results of a complex dynamics which depends on the density of the cells, their position, speed, orientation, geometry, etc. In the model of the T-cell population we are proposing, this complex dynamics is represented by the population event generator (PEG) block in Fig. 4. The PEG has as many outputs as micro-agents (the T-cells) and generates the event sequences $u_1, u_2, \ldots, u_N$ (see Fig. 4) in exactly the same way as they appear in the biological population. This is graphically depicted in Fig. 4 by the arrows pointing from the cells in the population to the micro-agent inputs. The introduction

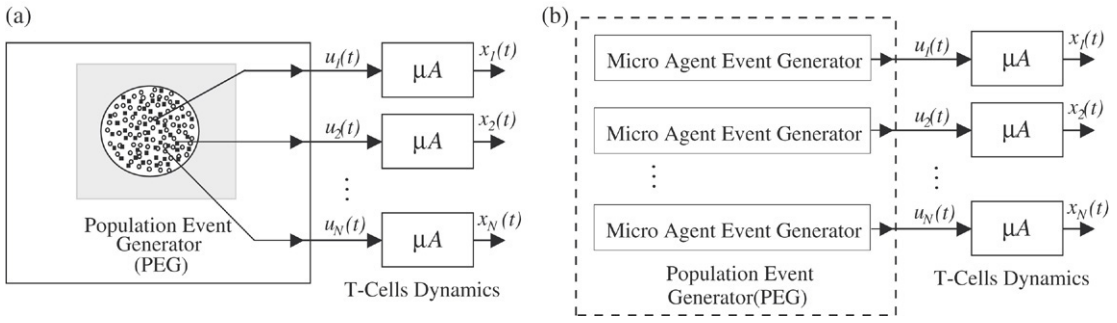

Fig. 4. The T-cell population model; (a) the hybrid system model u_i — event sequence input to the ith T-cell, x_i — the TCR expression of the ith T-cell, $i = 1, 2, \ldots, N$; (b) the population event generator (PEG) is decomposed into several micro-agent event generators (MAEG). The serial connection of MAEG and micro-agents is named a stochastic micro-agent, SμA.

of the PEG in the model makes a strong practical point in decomposing the cell population TCR expression dynamics into:

- a deterministic part (micro-agents), which describes the behavior of the individual T-cell TCR expression dynamics,
- a stochastic part, related to the complex dynamics of massive random encounters of T-cells and APCs (PEG).

The event generation depends on many population variables. An approach for modeling this complexity is applying a stochastic approach, *where the full complexity of interactions is described by the probability that an event happens*. The population we are considering consists of the individuals of the same nature and we expect the event sequences $u_i(t), i = 1, 2, \ldots, N$, generated by the PEG, to be of the same stochastic nature. If the event sequences are mutually independent, the PEG can be decomposed into the set of parallel micro-agent event generators (MAEG), as presented in Fig. 4. Each of the MAEGs produces an event sequence to the input of one micro-agent. We call the serial connection of MAEG and micro-agent a stochastic micro-agent (SμA; see Appendix B). The output of the SμA is a continuous time stochastic process (see Fig. 3).

The study of the connection between the individual microdynamics and the population macrodynamics is strongly related to statistical physics [8] where the behavior and the properties of mechanical bodies made up of a very large number of separate particles are studied. In this framework, the connection between the microdynamics and macrodynamics is established through the probability density function (pdf) of system particles over a state space. The pdf has a dual meaning. First, the pdf defines the probability of an individual particle being in a given state. Second, it represents the normalized frequency of the state occupancy by the particle population. Therefore, the state pdf can be considered as the population state.

Applying the same reasoning to our case, we can identify the state as the couple (x, q), which uniquely defines the state of an individual cell. The state pdf, i.e., the state of the population $\rho(x, t)$, is the vector of functions

$$\rho(x, t) = [\rho_1(x, t)\ \rho_2(x, t)\ \rho_3(x, t)]^{\mathrm{T}}. \tag{3}$$

In this vector, each component $\rho_q(x, t)$ is the probability of a cell with the expression level x in the discrete state q. The components of the state pdf are normalized, so that

$$\int_{-\infty}^{+\infty} \sum_{q=1}^{3} \rho_q(x, t)\mathrm{d}x = 1. \tag{4}$$

On the basis of the state pdf, the TCR expression distribution in the population can be computed as a total probability of cells with the expression level x independently on the discrete state, i.e.,

$$\eta(x, t) = \sum_{q=1}^{3} \rho_q(x, t). \tag{5}$$

This probability density function corresponds to experimentally obtained TCR-expression-associated fluorescence distributions obtained by flow cytometry.

We derive the stochastic micro-agent model of the T-cell, proposed here, from the previous deterministic micro-agent model (Fig. 2) defining $u(t)$ as the stochastic event sequence which produces stochastic transitions from the discrete state q to the discrete state r with stochastic rates λ_{qr}. In general, the rates can depend on t, but to make the notation simpler, we will drop the brackets, i.e., $\lambda_{qr} = \lambda_{qr}(t)$ (see Fig. 2). This assumption leads us to a continuous time Markov chain micro-agent (CTMCμA; see Appendix B), for which the evolution of the probability density function $\rho(x, t)$ of the T-cell hybrid state (x, q), $q = 1, 2, 3$, obeys the system of partial differential equations provided by the following theorem which is proved in Appendix C.

Theorem 1. *For a* CTMCμA *with N discrete states and discrete state probability satisfying*

$$\dot{P}(t) = L^{\mathrm{T}} P(t) \tag{6}$$

where $P(t) = [P_1(t)\ P_2(t) \dots P_N(t)]^{\mathrm{T}}$, P_q *is the probability of discrete state* q, $L = [\lambda_{qr}]^{\mathrm{T}}_{N\times N}$ *is a transition rate matrix and* λ_{qr} *is the rate of transition from discrete state* q *to discrete state* r*, the state pdf is given by the vector*

$$\rho(x, t) = [\rho_1(x, t), \rho_2(x, t), \dots, \rho_N(x, t)]^{\mathrm{T}} \tag{7}$$

where $\rho_q(x, t)$ *is the* pdf *of state* (x, q) *at time* t*, and satisfies the following equation:*

$$\frac{\partial \rho(x,t)}{\partial t} = L^{\mathrm{T}}\rho(x,t) - \begin{bmatrix} \nabla\cdot(f_1(x)\rho_1(x,t)) \\ \nabla\cdot(f_2(x)\rho_2(x,t)) \\ \vdots \\ \nabla\cdot(f_N(x)\rho_N(x,t)) \end{bmatrix} \tag{8}$$

where

$$\nabla\cdot(f_q(x)\rho_q(x,t)) = \sum_{j=1}^{n} \rho_q(x,t)\frac{\partial f_q^j(x)}{\partial x_j} + f_q^j \frac{\partial \rho_q(x,t)}{\partial x_j} \tag{9}$$

and $f_q^j(x)$ *is the* j*th component of vector field* $f_q(x)$ *at state* (x, q), $x \in X$, $X = R^n$, $q = 1, 2, \dots, N$. □

The PDE system (8) is an extension of Liouville's equation [8]. The solution of the partial differential equation (8) is the vector of the functions representing the time evolution of the CTMCμA state pdf. To solve this equation, the region $\Omega \in X$ and the boundary condition have to be defined [4]. An example of the boundary condition is $\rho(x, t) = 0$ for all $x \in \partial\Omega$. Specification of the boundary condition depends on the problem which is described by Eq. (8) and can strongly influence the solution [4]. The numerical methods for solving this type of equation are discussed in [20].

5. Example of the analytically predicted TCR expression distribution

To illustrate the previously described modeling approach, we will present possible predictions of the TCR expression pdf of the T-cells interacting with the APCs inside the lymph node. In the following analysis, we will assume that the transition rates of the proposed T-cell micro-agent model $\lambda_{12}, \lambda_{23}, \lambda_{32}$ are constant and that the continuous dynamics of discrete states are in the form of (1), where $f_1(x) = 0$, assuming that in the *never conjugated* state there is no change of TCR expression level.

Under these assumptions, the equation which describes the evolution of the state pdf of CTMCμA (see Appendix C) is

$$\frac{\partial \rho_1}{\partial t} = -\lambda_{12}\rho_1 - \frac{\partial}{\partial x}(f_1\rho_1) \tag{10}$$

$$\frac{\partial \rho_2}{\partial t} = \lambda_{12}\rho_1 - \lambda_{23}\rho_2 + \lambda_{32}\rho_3 - \frac{\partial}{\partial x}(f_2\rho_2) \tag{11}$$

$$\frac{\partial \rho_3}{\partial t} = \lambda_{23}\rho_2 - \lambda_{32}\rho_3 - \frac{\partial}{\partial x}(f_3\rho_3), \tag{12}$$

where $\rho_i = \rho_i(x, t)$ and the pdf of TCR expression is given by

$$\eta(x, t) = \rho_1 + \rho_2 + \rho_3. \tag{13}$$

For the given initial TCR expression pdf of naive cells, this set of equations can be used to predict the TCR expression pdf evolution over time. This time evolution can be compared to experimental TCR expression distributions obtained by flow cytometry. This type of analysis is given in the next section.

However, we can also solve this equation at steady state, i.e., taking the limit, $t \to \infty$. Using this limit, we can derive the steady-state pdf of the TCR expression. For the steady state, the expressions (10)–(12) are

$$0 = -\lambda_{12}\rho_1^s - \frac{\partial}{\partial x}(f_1\rho_1^s) \tag{14}$$

$$0 = \lambda_{12}\rho_1^s - \lambda_{23}\rho_2^s + \lambda_{32}\rho_3^s - \frac{\partial}{\partial x}(f_2\rho_2^s) \tag{15}$$

$$0 = \lambda_{23}\rho_2^s - \lambda_{32}\rho_3^s - \frac{\partial}{\partial x}(f_3\rho_3^s), \tag{16}$$

where $\rho_i^s = \rho_i^s(x)$. Since $f_1 = 0$ (see Eq. (2)), we can conclude that $\rho_1^s(x) = 0$ and can transform the system of equations (14)–(16) to the equivalent

$$0 = -\lambda_{23}\rho_2^s + \lambda_{32}\rho_3^s - \frac{\partial}{\partial x}(f_2\rho_2^s) \tag{17}$$

$$0 = \frac{\partial}{\partial x}(f_2\rho_2^s + f_3\rho_3^s) \Leftrightarrow f_2\rho_2^s + f_3\rho_3^s = \text{const.} \tag{18}$$

Since the probability functions $\rho_i^s(x)$ cannot be negative $\rho_i^s(x) \geq 0, \forall x \in R$, and the TCR expression is greater than zero ($x \geq 0$), we know that $\rho_2(0^-) = \rho_3(0^-) = 0$. Therefore, the system of equations (17) and (18) becomes

$$0 = -\lambda_{23}\rho_2^s + \lambda_{32}\rho_3^s - \frac{\partial}{\partial x}(f_2\rho_2^s) \tag{19}$$

$$0 = f_2\rho_2^s + f_3\rho_3^s. \tag{20}$$

After substituting $\rho_3^s(x) = \eta^s(x) - \rho_2^s(x)$, the solution for the steady state of Eqs. (10)–(13) is equivalent to the solution of the following differential equation:

$$\frac{\mathrm{d}\eta^s}{\mathrm{d}x} = -\left[\left(\frac{f_3 f_2}{f_3 - f_2}\right)^{-1}\frac{\mathrm{d}}{\mathrm{d}x}\left[\frac{f_3 f_2}{f_3 - f_2}\right] + \frac{\lambda_{23}}{f_2} + \frac{\lambda_{32}}{f_3}\right]\eta^s. \tag{21}$$

The function $\eta^0(x)$, which satisfies this differential equation for $\eta^s(x) = \eta^0(x)$, is

$$\eta^0(x) = c\left|\frac{1}{f_3(x)} - \frac{1}{f_2(x)}\right| \mathrm{e}^{-\int(\frac{\lambda_{23}}{f_2(x)} + \frac{\lambda_{32}}{f_3(x)})\mathrm{d}x} \tag{22}$$

where c is the normalization parameter. This equation defines the shape of the steady-state TCR expression pdf. This result is very important, as it explicitly shows that the TCR expression pdf shape depends on the TCR expression dynamics of the individual cells, described by functions f_2 and f_3. To obtain the expression for the steady-state TCR expression pdf, we should be careful with the integration in the exponent of Eq. (22), dependent on functions f_2 and f_3.

To illustrate the solution (22), we will consider a very simple TCR expression level dynamics in *conjugated* and *free* states:

$$f_2(x) = S_2 - k_2 x < 0; \qquad f_3(x) = S_3 - k_3 x \geq 0. \tag{23}$$

In the conjugated state, the TCR expression $x(t)$ declines, while in the free state $x(t)$ can incline or remain constant. The consequence of (23) is that the T-cell which is always in a *conjugated* or *free* state will express $x_a = S_2/k_2$ and $x_b = S_3/k_3$ TCRs, respectively. It is reasonable to assume that x_a and x_b are the limits of the region with non-zero TCR expression pdf at the steady state, i.e., the steady-state pdf $\eta^s(x)$ satisfies

$$\eta^s(x) = \begin{cases} 0, & x \in (-\infty, x_a] \cup [x_b, \infty) \\ \eta^0(x), & x \in (x_a, x_b) \end{cases} \tag{24}$$

where the normalization parameter c (17) is such that $\int_{x_a}^{x_b} \eta^s(x)\mathrm{d}x = 1$. The mathematical development below is applied only to the interval $x \in (x_a, x_b)$, where $\eta^s(x) \neq 0$.

Substituting (23) in Eq. (22), we obtain

$$\eta^s(x) = c \left| \frac{1}{S_3 - k_3 x} + \frac{1}{k_2 x - S_2} \right| \mathrm{e}^{-\int (\frac{\lambda_{23}}{S_2 - k_2 x} + \frac{\lambda_{32}}{S_3 - k_3 x})\mathrm{d}x} \tag{25}$$

and then, computing integrals in the exponential terms,

$$\eta^s(x) = c \left| \frac{1}{S_3 - k_3 x} + \frac{1}{k_2 x - S_2} \right| \mathrm{e}^{\frac{\lambda_{23}}{k_2} \ln|S_2 - k_2 x| + \frac{\lambda_{32}}{k_3} \ln|S_3 - k_3 x|} \tag{26}$$

and applying an algebraic transformation to the logarithmic terms results in

$$\eta^s(x) = c_1 \left| \frac{k_3/k_2}{S_3/k_3 - x} + \frac{1}{x - S_2/k_2} \right| (x - S_2/k_2)^{\frac{\lambda_{23}}{k_2}} (S_3/k_3 - x)^{\frac{\lambda_{32}}{k_3}} \tag{27}$$

where the normalization parameter c_1 is introduced because of the algebraic transformations. Finally, substituting $x_a = S_2/k_2$ and $x_b = S_3/k_3$, we obtain

$$\eta^s(x) = c_1 \left[\frac{k_3}{k_2} (x - x_a)^{\left(\frac{\lambda_{23}}{k_2} - 1\right)} (x_b - x)^{\frac{\lambda_{32}}{k_3}} + (x - x_a)^{\frac{\lambda_{23}}{k_2}} (x_b - x)^{\left(\frac{\lambda_{32}}{k_3} - 1\right)} \right]. \tag{28}$$

The shape of the $\eta^s(x)$ in the interval $x \in (x_a, x_b)$, $0 \leq x_a < x_b$ depends on x_a, x_b, and the ratios λ_{23}/k_2 and λ_{32}/k_3. The points x_a and x_b are the potential singular points of the function (28). The presence of a singular point means that the steady-state pdf at that point is a Dirac pulse. Singularity at the point x_a appears if the ratio $\lambda_{23}/k_2 < 1$. Similarly, the singularity at the point x_b appears if the ratio $\lambda_{32}/k_3 < 1$. If the singularity at the points x_a or x_b does not exist, then $\lambda_{23}/k_2 > 1$ and $\lambda_{32}/k_3 > 1$.

It is worth mentioning that if we replace variable x with

$$x = \alpha x_a + (1 - \alpha) x_b, \quad \alpha \in [0, 1] \tag{29}$$

the expression (28) becomes

$$\eta^s(x = \alpha x_a + (1 - \alpha) x_b) = \frac{k_3}{k_2 + k_3} \beta\left(\frac{\lambda_{23}}{k_2}, \frac{\lambda_{32}}{k_3} + 1\right) + \frac{k_2}{k_2 + k_3} \beta\left(\frac{\lambda_{23}}{k_2} + 1, \frac{\lambda_{32}}{k_3}\right) \tag{30}$$

where β is the so-called beta probability density function given by Papoulis [13]:

$$\beta(\alpha | p, q) = \frac{1}{B(p, q)} \alpha^{p-1} (1 - \alpha)^{q-1} \tag{31}$$

and $B(p, q)$ is the special function Beta for parameters p and q.

The probability density function derived above is a weighted sum of two Beta pdfs. Beta pdf can have very different shapes depending on its parameters. For example, it includes the shape of the uniform distribution ($p = q = 1$), the symmetric unimodal pdf ($p = q$), and an asymmetric distribution which may look like an exponential distribution ($p = 1$ and $q \gg p$, or $q = 1$ and $p \gg q$), where symbols $\gg$ and $\ll$ denote the relations *much greater* and *much smaller*, which are, in practice, 10 times greater and 10 times smaller. Finally, the Beta pdf can take an asymmetric shape similar to a log-normal distribution ($p, q > 1$ and $p \gg q$ or $p \ll q$), which is frequently found in experimental histograms of the receptor-associated fluorescence intensity [17]. This illustrates how the shape of the distributions can be used to assess different hypotheses, even when the precise parameter values cannot be or have not been estimated. It also emphasizes that interpreting the experimental observation of the symmetric distribution of the log-TCR expression as a true log-normal distribution might be unwarranted.

From this example, we learn that the correct interpretation of experimental distributions requires an insight into stochastic interactions of individual cells. But, more important, the example shows that the shape of experimental distributions is the point where questions about the individual cell dynamics can be investigated.

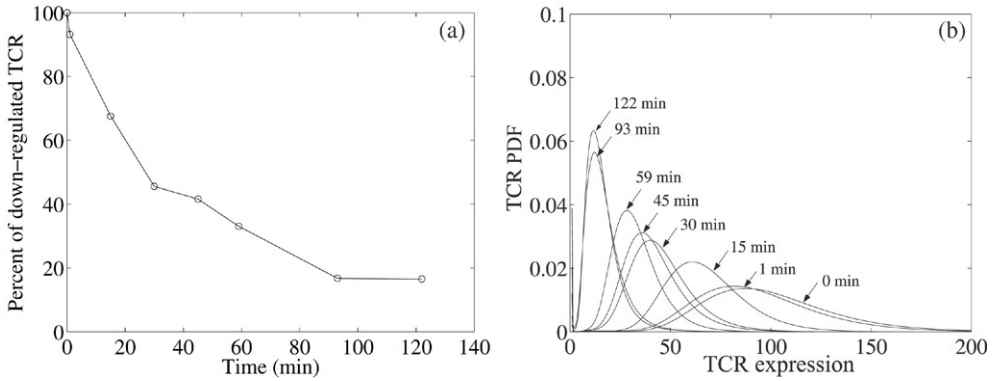

Fig. 5. Experimental data [9]: (a) the mean value of down-regulated TCR, (b) TCR expression pdfs $\eta_{\exp}(x, t_j)$, $j = 1, 2, \ldots, 8$.

6. Relation to previous works

Using the time record of TCR distribution mean values, Bachmann et al. [1] analyze dynamics of the TCR down-regulation. The data are from the experiment where T-cells remain conjugated with APCs all the time. Two hypotheses are considered: linear and quadratic. According to the linear hypothesis, each TCR molecule is down-regulated after the interaction with a single ligand (MHC/peptide complex) expressed on the APC surface and the dynamics of individual cell down-regulation during the conjugation is

$$f_2(x) = -k_2 x. \tag{32}$$

By the quadratic hypothesis, TCR and ligands must form couples (dimers) before down-regulation and the dynamics of down-regulation of the single cell is

$$f_2(x) = -k_2 x^2. \tag{33}$$

By [1], the quadratic hypothesis is more appropriate. Sousa and Carneiro [15] using the data of Valitutti et al. [17] extended linear and quadratic hypotheses in order to find a better agreement of the model with the data. On the other hand, more recently, Wofsy et al. [18] developed the stochastic model of serial TCR–ligand interaction, and comparing with the Valitutti et al. [17] data found the linear hypothesis more convincing. However, because of the saturation in the data, similar to the one present in Fig. 5(a), their linear hypothesis includes an extra constant term provided that the TCR expression does not go to zero when $t \to \infty$.

Here we are analyzing the data from the experiment of Lino [9] which is similar to the previous experiments [17,1]. In this experiment, the T-cell population is exposed to a large amount of *antibodies*. The T-cell suspension is added to a solution of antibodies and stirred in seconds. Under these conditions, we can assume that all T-cells are immediately "conjugated" since at the beginning of the experiment they are exposed to the antibodies that play the role of ligands expressed on the APC surface. Thus, all of the T-cells in the population are in the single *conjugated* state. Expecting that the T-cells react in the same way either to APC or antibodies, this experiment provides us with a source of data that can be used to identify the dynamics of the individual T-cell dynamics in the *conjugated* state, i.e., the individual T-cell TCR decrease dynamics.

In the case of always conjugated T-cells, by our modeling approach, the TCR expression distribution evolution is described by a single partial differential equation for $\rho_2(x, t)$, the so-called Liouville equation:

$$\frac{\partial \rho_2(x,t)}{\partial t} = -\nabla \cdot (f_2(x)\rho_2(x,t)), \tag{34}$$

where according to the notation of the previous section, the TCR expression distribution $\eta(x, t) = \rho_2(x, t)$ and $\rho_1(x, t) = \rho_3(x, t) = 0$. The experimentally estimated TCR expression pdf $\eta_{\exp}(x, t)$ evolution obtained from our T-cell–antibody experiment is presented in Fig. 5(b) [12]. The TCR expression pdf is estimated at $t_1 = 0$, $t_2 = 1$, $t_3 = 15$, $t_4 = 30$, $t_5 = 45$, $t_6 = 59$, $t_7 = 93$ and $t_8 = 122$ min, after the experiment start.

To test the hypothesis of the linear and the quadratic models of the individual T-cell TCR down-regulation dynamics, we will compare the evolution of the predicted TCR expression pdf $\eta(x, t) = \rho_2(x, t)$ using (34) to

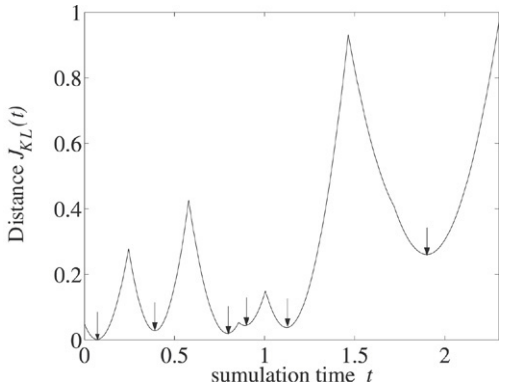

Fig. 6. The distance $J_{\mathrm{KL}}(t)$ computed for the linear hypothesis. Local minima signaled by arrows correspond to the time instants τ_k when $\eta(x,t)$ is close to some of the experimental TCR pdfs, $\eta_{\exp}(x,t_j)$, $j=1,2,\ldots,8$.

the experimentally obtained TCR expression pdf $\eta_{\exp}(x,t_j)$, $j=1,2,\ldots,8$. The initial condition for the prediction is $\rho_2(x,0)=\eta_{\exp}(x,0)$. The shape of the evolution $\eta(x,t)$, calculated using (34) at different times, does not depend on parameter k_2, either for the linear or for the quadratic hypothesis, because the parameter k_2 in Eq. (34), for both *linear* and *quadratic* cases, only scales the time. This allows us to take $k_2=1$ and compare the shapes in prediction $\eta(x,t)$ to the shapes in experimental data $\eta_{\exp}(x,t_j)$. Using $k_2=1$, we should keep in mind that the time used in prediction t and the time in experiment t_j are not measured in the same time frame.

To compare the shape of prediction $\eta(x,t)$ to experimental data $\eta_{\exp}(x,t_j)$ we need to choose the times $\tau_k, k=1,2,\ldots$, at which we are comparing $\eta(x,t=\tau_k)$ to $\eta_{\exp}(x,t_j)$. We determine τ_k as the times when the model predicted pdf $\eta(x,t)$ is most similar to some of the experimentally obtained pdfs $\eta_{\exp}(x,t_j)$, $j=1,2,\ldots,8$. To find τ_k, we use the distance which compares the pdfs in terms of Kullback–Leibler (KL) distance [3]:

$$J_{\mathrm{KL}}(\eta(t),\eta_{\exp})=\min_j \sum_i \eta(x_i,t)\log\frac{\eta(x_i,t)}{\eta_{\exp}(x_i,t_j)} \tag{35}$$

which measures the distance between the predicted pdf at time t, $\eta(x,t)$, and the set of experimentally obtained measurements $\eta_{\exp}$, computed as the minimal value of the KL distance between $\eta(x,t)$ and $\eta_{\exp}(x,t_j)$, $j=1,2,\ldots,8$. The KL distance is the entropy based distance used commonly to measure the similarity between two pdfs. The distance $J_{\mathrm{KL}}(\eta(t),\eta_{\exp})$ computed for the linear hypothesis pdf prediction is presented in Fig. 6. It is small whenever $\eta(x,t)$ is similar to some of the $\eta_{\exp}(x,t_j)$, $j=1,2,\ldots,8$. Therefore, the time instants $\tau_k, k=1,2,\ldots$, correspond to the local minima of $J_{\mathrm{KL}}(\eta(t),\eta_{\exp})$, which are signaled by the arrows in Fig. 6.

The TCR expression pdf evolution for the linear hypothesis, calculated using (34) at time instants $\tau_k, k=1,2,\ldots,6$, is plotted in Fig. 7(a). From the figure, we can see that the shape of the $\eta(x,t)$ evolution according to the linear hypothesis matches the shape of the experimental TCR pdf well.

A similar analysis can be made for the quadratic hypothesis. However, this makes little sense, since in the quadratic case, the TCR expression pdf evolution does not produce shapes of $\eta(x,t)$ which approximate closely the experimental TCR expression pdf (Fig. 7(b)).

On the basis of just the shapes in the $\eta(x,t)$ evolution, we can conclude that the individual T-cell TCR down-regulation dynamics of the *conjugated state* is closer to the linear hypothesis.

7. Discussion

In this paper, the TCR expression distribution dynamics of a T-cell population interacting with ligand-bearing APCs is studied. Each individual T-cell is described by a deterministic micro-agent model, which is defined in the hybrid automata framework. Under a stochastic assumption about the micro-agent input event sequence, the stochastic micro-agent model of the T-cell population is introduced. The use of the relationship between the proposed model and the time evolution of the state pdf provides us with the possibility of predicting experimental TCR expression distributions.

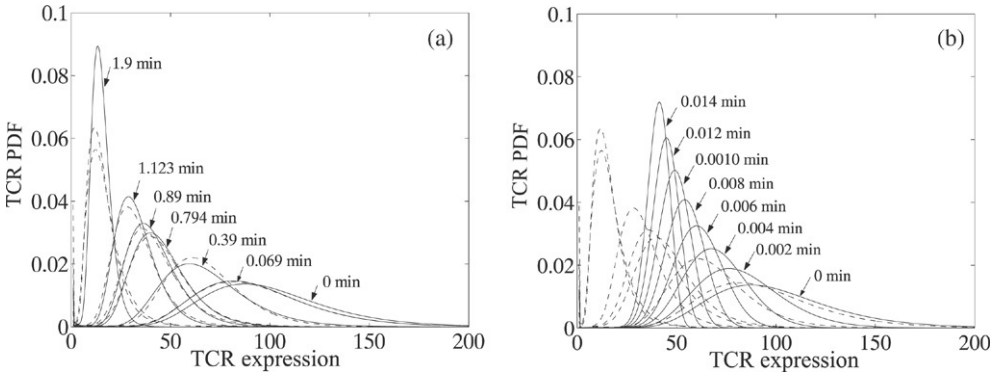

Fig. 7. Time evolution of TCR pdf, linear hypothesis, (a) model predicted $\eta(x,t)$ (*solid*, computed at time τ_k), the experimental TCR pdf $\eta_{\exp}(x,t_j)$ (*dashed*), $j = 1,2,\ldots,8$, time evolution of the TCR pdf, quadratic hypothesis, (b) model predicted $\eta(x,t)$ (*solid*), the experimental TCR pdf $\eta_{\exp}(x,t_j)$ (*dashed*), $j = 1,2,\ldots,8$.

We have made a few simplifications that are not free from controversy on biological grounds. First, we have assumed that conjugate lifetimes and waiting times for the conjugation are both exponentially distributed, which leads to the Markov chain model for the discrete state sequence. This assumption is reasonable for the waiting time, since T-cells and APCs seem to be involved in random walks. As to the distribution of conjugate lifetimes, it seems to be akin to an exponential under some experimental settings [5,10], while in other conditions it is more bell-shaped, with the mean value of a few hours [6].

Potential future theoretical work along these research lines includes an extension to T-cell population dynamics, in which life-history parameters (such as rates of death and proliferation) are themselves functions of the TCR signaling [16,2]. The initial and steady-state distributions could be more carefully studied using better approximations, or including better hypotheses about the TCR expression dynamics in the absence of APCs, and extra sources of the variance in the TCR expression distribution. On experimental grounds, it would be interesting to test the proposed model using *in vivo* experimentally obtained data. Such data could be obtained from the two-photon microscopy observations inside the lymph node and corresponding TCR expression measurements.

In this paper, we used the TCR down-regulation as an example of where hybrid dynamics occurs. However, the theory presented here could be used to provide additional insights into other biological phenomena, where cells or other biological agents alternate among discrete states. In some sense, we are challenging the research community to consider the shapes of the probability density functions, estimated from population measurements, as a place where they can investigate individual interactions inside the population of the immune system cells.

Acknowledgements

The work was supported by Foundation for Science and Technology (Portugal): a fellowship to DM (SFRH/BD/2960/2000), and a grant to JC (POCTI/MGI/46477/2002 with FEDER funds). We would also like to thank Prof. Rob de Boer, Utrecht University, Utrecht, The Netherlands, for the welcome support he gave us along the way.

Appendix A. Hybrid automaton used for the micro-agent individual model

Definition 2 (*[14]*). A hybrid automaton H is a collection $H = (Q, X, \text{Init}, f, \text{Inv}, E, G, \text{Rs})$, where:

- Q is a finite set of discrete states,
- $X \subseteq R^n$ the continuous state space,
- $\text{Init} \subseteq Q \times X$ is the set of initial states,
- $f : Q \times X \to TX$ assigns to each $q \in Q$ a vector field $f_q(x)$,
- $\text{Inv} : Q \to 2^X$ assigns to each $q \in Q$ an invariant set; as long as the discrete state is $q \in Q$, the continuous state $x \in \text{Inv}(q)$,
- $E \subseteq Q \times Q$ is a collection of edges (discrete transitions),

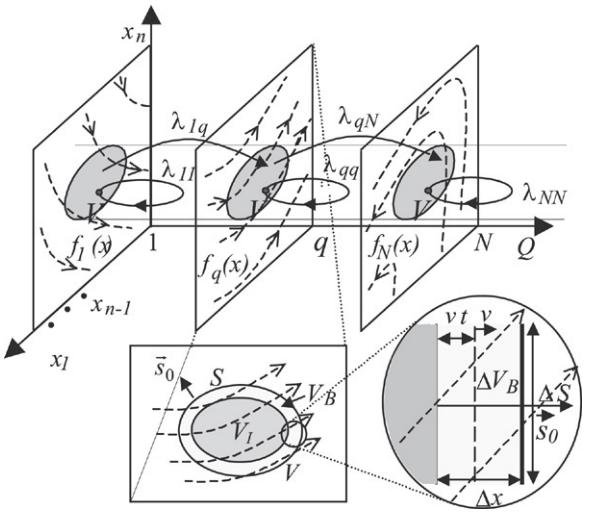

Fig. C.1. Possible trajectories in the micro-agent state space: x_j — components of the continuous state x, q — state of the discrete space, $f_q(x)$ — vector field corresponding to q, V — trajectory volume, V_I — volume of trajectories not crossing the surface S in the time interval $[t, t + \Delta t)$, V_B — volume of trajectories crossing surface S in the time interval $[t, t + \Delta t)$, ΔV_B — element of the volume V_B, ΔS — element of the surface S, v — projection of the vector field $f_q(x)$ onto the surface vector $\vec{s}_0$, Δx — length $v\Delta t$.

- $G : E \to 2^X$ assigns to $e \in E$ a guard set, representing the collection of the discrete transitions allowed by the state vector,
- $\mathrm{Rs} : X \times E \to X$ assigns to $e \in E$ and $x \in X$ a reset map, describing jumps in the continuous state space due to the event e.

Appendix B. Stochastic micro-agent

Definition 3 (*[7] Micro-agent Stochastic Execution*). A stochastic process $(x(t), q(t)) \in X \times Q$ is called a *micro-agent stochastic execution* if and only if a micro-agent stochastic input event sequence $e(\tau_n), n \in N, \tau_0 = 0 \leq \tau_1 \leq \tau_2 \leq \cdots$, generates transitions in such a way that in each interval $[\tau_n, \tau_{n+1}), n \in N, q(t) \equiv q(\tau_n)$.

Remark 2. The $x(t)$ of a stochastic execution is a continuous time function since the transition changes only the discrete state of a micro-agent.

Definition 4 (*Stochastic Micro-agent,* SμA). A stochastic micro-agent is a pair $\mathrm{S\mu A} = (\mu\mathrm{A}, e(t))$, where μA is a micro-agent and $e(t)$ is a micro-agent stochastic input event sequence such that the stochastic process $(x(t), q(t)) \in X \times Q$ is a micro-agent stochastic execution.

Definition 5 (*Micro-agent Continuous Time Markov Chain Execution*). A micro-agent stochastic execution $(x(t), q(t)) \in X \times Q$ is called a micro-agent continuous time Markov chain execution iff the input stochastic event sequence $e(\tau_n), n \in N, \tau_0 = 0 \leq \tau_1 \leq \tau_2 \leq \cdots$ generates transitions whose conditional probability satisfies $P[q(\tau_{k+1}) = q_{k+1} | q(\tau_k) = q_k, q(\tau_{k-1}) = q_{k-1}, \ldots q(\tau_0) = q_0] = P[q(\tau_{k+1}) = q_{k+1} | q(\tau_k) = q_k]$.

Remark 3. The $q(t)$ of a micro-agent continuous Markov chain execution is a continuous time Markov chain.

Definition 6. Continuous time Markov chain micro-agent, CTMCμA. A stochastic micro-agent is called a continuous time Markov chain micro-agent iff $(x(t), q(t)) \in X \times Q$ is a micro-agent continuous time Markov chain execution.

Appendix C. Proof of Theorem 1

The state space $X \times Q$ of the stochastic micro-agent is presented in Fig. C.1. The transition between the discrete states is a continuous time Markov chain stochastic process and $x(t)$ is a continuous time function, i.e.,

$x(t^-) = x(t^+) = x(t)$. The probability $p_{V,q}$ that micro-agent state $(x, q) \in \{(x, q)|x \in V\}$ is given by

$$p_{V,q} = \int_V \rho_q(x, t)\mathrm{d}V, \tag{C.1}$$

where $\rho_q(x)$ is the probability density function of the state (x, q) and an arbitrarily chosen volume V in X. The time derivative of $p_{V,q}$ is

$$\dot{p}_{V,q}(t) = \int_V \frac{\partial \rho_q(x, t)}{\partial t}\mathrm{d}V. \tag{C.2}$$

Using Fig. C.1. the time derivative of $p_{V,q}$ can be written as

$$\dot{p}_{V,q}(t) = \lim_{\Delta\to 0} \frac{1}{\Delta t}\left[\Delta p_{V_I} + \sum_{S,\Delta S\to 0} \Delta p_{\Delta S\Delta x}\right], \tag{C.3}$$

where Δp_{V_I} and $\Delta p_{\Delta S\Delta x}$ are probability changes in the volumes V_I and $\Delta V_B = \Delta S\Delta x$, respectively, and $V_B = \sum_{S,\Delta S\to 0} \Delta S\Delta x$. Due to the continuity of $x(t)$

$$\lim_{\Delta t\to 0} \frac{1}{\Delta t}\Delta p_{V_I} = \sum_{r=1}^{N} \lambda_{rq} \int_{V_I} \rho_q(x)\mathrm{d}V \tag{C.4}$$

since in the time interval $[t, t + \Delta t)$, $x(t)$ does not leave volume V_I and probability in V_I changes due to the Markov chain transitions. During the same interval, the increase of probability in the volume $\Delta V_B = \Delta S\Delta x$ is

$$\Delta p_{\Delta S\Delta x}(t) = -\Delta S\left[\int_t^{t+\Delta t} v\rho_q(x, \tau) + \dot{\rho}_q(x, \tau)(\Delta x - v\tau)\mathrm{d}\tau\right], \tag{C.5}$$

where $x \in \Delta V_B$. Taking into account the Markov chain transitions in the volume ΔV_B and Eq. (C.4), we have

$$\lim_{\Delta t\to 0} \frac{\Delta p_{\Delta S\Delta x}(t)}{\Delta t} = -\Delta S v\rho_q(x, \tau) + \Delta x \sum_{r=1}^{N} \lambda_{rq}\rho_r(x, t). \tag{C.6}$$

Substituting (C.4) and (C.6) into (C.3) gives

$$\dot{p}_{V,q}(t) = \sum_{r=1}^{N} \lambda_{rq} \int_{V_I} \rho_q(x, t)\mathrm{d}V + \sum_{\Delta S,\Delta S\to 0}\left[-\Delta S v\rho_q(x, t) + \Delta S\Delta x \sum_{r=1}^{N} \lambda_{rq}\rho_r(x, t)\right], \tag{C.7}$$

i.e.,

$$\dot{p}_{V,q}(t) = \sum_{r=1}^{N} \lambda_{rq} \int_V \rho_q(x, t)\mathrm{d}V - \oint_S f_q(x)\rho_q(x, t)\mathrm{d}S. \tag{C.8}$$

With the use of Gauss's theorem, we obtain

$$\dot{p}_{V,q}(t) = \int_V \left[\sum_{r=1}^{N} \lambda_{rq}\rho_q(x, t) - \nabla \cdot (f_q(x)\rho_q(x, t))\right]\mathrm{d}V. \tag{C.9}$$

Taking the small volume limit of the Eqs. (C.2) and (C.9), we have

$$\frac{\partial \rho_q(x, t)}{\partial t} = \sum_{r=1}^{N} \lambda_{rq}\rho_q(x, t) - \nabla \cdot (f_q(x)\rho_q(x, t)). \tag{C.10}$$

Using $\rho(x,t) = [\rho_1(x,t), \rho_2(x,t), \ldots, \rho_N(x,t)]^{\mathrm{T}}$, the equation system (C.10) becomes

$$\frac{\partial \rho(x,t)}{\partial t} = L^{\mathrm{T}}\rho(x,t) - \begin{bmatrix} \nabla \cdot (f_1(x)\rho_1(x,t)) \\ \nabla \cdot (f_2(x)\rho_2(x,t)) \\ \vdots \\ \nabla \cdot (f_N(x)\rho_N(x,t)) \end{bmatrix}. \quad \square \tag{C.11}$$

References

[1] M.F. Bachmann, M. Salzmann, A. Oxenius, P.S. Ohashi, Formation of TCR dimers/trimers as a crucial step for T cell activation, Eur. J. Immunol. 28 (1998) 2571–2579.

[2] J. Carneiro, T. Paixão, D. Milutinovic, J. Sousa, K. Léon, R. Gardner, J. Faro, Immunological self-tolerance: Lessons from mathematical modeling, J. Comput. Appl. Math. 184 (2005) 77–100.

[3] C. Cover, J. Thomas, Elements of Information Theory, John Wiley, New York, 1991.

[4] L.C. Evans, Partial Differential Equations, American Mathematical Society, Providence, 1998.

[5] M. Gunzer, A. Schafer, et al., Antigen presentation in extracellular matrix: Interactions of T cells with dendritic cells are dynamic, short lived, and sequential, Immunity 13 (3) (2000) 323–332.

[6] J.B. Huppa, M.M. Davis, T-cell–antigen recognition and the immunological synapse, Nat. Rev. Immunol. 3 (12) (2003) 973–983.

[7] H. Jianghai, J. Lygeros, S. Sastry, Towards a Theory of Stochastic Hybrid Systems, HSCC Springer-Verlag, 2000, pp. 160–173.

[8] L.D. Landau, E.M. Lifshitz, Statistical Physics, Pergamon Press, 1959.

[9] A. Lino, Caracterização do mecanismo molecular de activação de linfocitos T, Relatório Final de Curso Bioqimica, Faculdade de Ciências da Univesidade de Lisboa, Lisboa, 2000, p. 47.

[10] T.R. Mempel, S.E. Henrickson, U.H. von Andrian, T-cell priming by dendritic cells in lymph nodes occurs in three distinct phases, Nature 427 (2004) 154–159.

[11] D. Milutinović, J. Carneiro, M. Athans, P. Lima, A hybrid automata model of TCR triggering dynamics, in: Proceedings of the 11th Mediterranean Conference on Control and Automation MED 2003, June 18–20, Rhodes, Greece, 2003.

[12] D. Milutinović, Stochastic model of micro-agents populations, Ph.D. Thesis, Instituto Superior Tecnico, Technical University of Lisbon, Portugal, 2004.

[13] A. Papoulis, Probability, Random Variables, and Stochastic Processes, McGraw-Hill, Inc., 1965.

[14] A. Schaft, H. Schumacher, An Introduction to Hybrid Dynamical Systems, in: Lecture Notes in Control and Information Sciences, vol. 251, Springer, 2000.

[15] J. Sousa, J. Carneiro, A mathematical analysis of TCR serial triggering and down-regulation, Eur. J. Immunol. 30 (2000) 3219–3227.

[16] J. Sousa, Modeling the antigen and cytokine receptors signaling processes and their propagation to lymphocyte population dynamics, Ph.D. Thesis, University of Lisbon, Lisbon, 2003, p. 161.

[17] S. Valitutti, S. Muller, et al., Serial triggering of many T-cell receptors by a few peptide–MHC complexes, Nature 375 (6527) (1995) 148–151.

[18] C. Wofsy, D. Coombs, B. Goldstein, Calculations show substantial serial engagement of T cell receptors, Biophys. J. 80 (2) (2001) 606–612.

[19] C. Wofsy, B. Goldstein, Effective rate models for receptors distributed in a layer above a surface: Application to cells and biacure, Biophys. J. 82 (4) (2002) 1743–1755.

[20] O.C. Zienkiewitz, R.L. Taylor, The Finite Element Method, in: Fluid Dynamics, vol. 3, Butterworth–Heinemann, 2000.